PROCEEDINGS OF SCIENCE

Resolving Dark Matter Tension: The impact of dynamical friction due to fuzzy dark matter on satellites with non-spherically symmetric potentials

Konstantinos N. Gourgouliatos[a,*] **and Andreas Vitsos**[a]

[a] [1]*Department of Physics, University of Patras, Patras, Rio, 26504, Greece*

E-mail: kngourg@upatras.gr

A possible candidate for dark matter is an ultralight bosonic particle comprising the Fuzzy Dark Matter (FDM). The presence of FDM in a galactic cluster will impact the motion of satellites residing in such clusters, through dynamical friction. Here we present numerical simulations of the dynamical friction on satellites traversing an initially uniform FDM halo. The potentials of the satellites we have studied are non-spherically symmetric and logarithmic. We find that the wakes created on the FDM halo due to the passage of such satellites are qualitatively different from those generated by spherically symmetric systems and we quantify the impact of fuzzy dark matter on the dynamical friction coefficient of the satellites.

Corfu Summer Institute 2022 "School and Workshops on Elementary Particle Physics and Gravity", 28 August - 1 October, 2022
Corfu, Greece

*Speaker

PoS(CORFU2022)246

Contents

1. Introduction

The existence of dark matter has been proposed by Zwicky [1] by application of the Virial Theorem to clusters of galaxies, at the realisation that members of clusters have higher velocities compared to what it would have been expected based on the light-emitting mass. Dark matter participates in the gravitational interaction but does not absorb nor emits any light, thus remains invisible. Rotation curves of galaxies [2] revealed a discrepancy between the light-emitting mass galaxies and the mass responsible for the gravitational interaction. The latter extends to larger distances from the centre compared to baryonic mass that interacts electomagnetically and creates a halo of dark matter. Further evidence of the existence of dark matter [3] include gravitational lensing [4], fluctuations of the Cosmic microwave background radiation [5] and galaxy cluster interaction [6], baryonic acoustic oscillations [7], to name just a few.

While dark matter corresponds to 26.4% of the energy content of the Universe [8], its nature is elusive. Numerous models have been proposed for the interpretation of dark matter, either in particle form, such as the weakly interacting massive particle [9], macroscopic massive objects, such as primordial black holes [10] or massive compact halo objects [11], neutrinos [12] or modified gravity [13]. Ultralight bosonic particles are rising candidates for dark matter, as proposed in [14]. These models cover a wide mass spectrum from the axion range up to 10^{-24}eV [15], within the general category of weakly interacting sub-electronvolt particle (WISPs) [16]. Fuzzy dark matter (FDM) [17], whose mass is in the range of $10^{-22} - 10^{-21}$eV, with a characteristic de Broglie length scale of a few kiloparsecs, is postulated to exhibit quantum effects on large scales due to its low mass. This wave-like behavior is predicted to have significant effects on the structure of dark matter halos, potentially resolving some of the outstanding issues with the cold dark matter model, such as the formation of too many small galaxies, the missing satellite problem [18] and the overly dense central regions of dark matter halos, the so-called core-cusp problem [19]. The cold nature of the particles allows for the formation of a Bose-Einstein condensate, which demonstrates a fluid-like behaviour, where Dynamical effects can occur.

A massive object moving within a mass concentration will experience dynamical friction, which is a drag due to gravity, as it has been formulated by Chandrasekhar [20–22]. This interaction decelerates the massive object, but also impacts the FDM halo creating smaller-scale structures [23] depending on the detailed properties of the FDM model employed. These effects have been studied analytically and numerically, considering the drag on a point mass and a spherically symmetric extended mass distribution, corresponding to the Plummer potential [24, 25]. However, given that massive objects, such as galaxies that play the role of satellites within FDM halos, are not necessarily spherically symmetric, it is possible that the drag and the wake generated on the shape of the object depend on their shape and orientation. Thus, we study here the impact of FDM to non-spherically symmetric objects, such as galaxies described by the axisymmetric logarithmic potentials. We simulate their evolution applying the methodology formulated in [24], and we compared against known systems that may be host FDM haloes.

The structure of this contribution is as follows. In section 2 we present equations describing FDM and the numerical scheme used for the study of the problem. In section 3 we present the simulations. Section 4 focuses on the results of the simulations. We conclude in the final section 5.

2. Mathematical Formulation

FDM exhibits quantum mechanical behaviour, which because of the very low particle mass has a corresponding de Broglie wavenumber that extends to astrophysical scales. Thus we shall use the Schrödinger equation for the basic dynamics. Moreover, we will be focusing on the gravitational dynamics, thus, we will be using the Poisson equation to find the relevant gravitational potential. The combination of these two, leads to the Schrödinger-Poisson equation. However, in the application we are discussing here, we will assume that the potential of the satellite dominates over the fuzzy dark matter potential, thus in the evolutionary equation we will using the Schoödinger equation for a particle of mass m within a potential U_s:

$$i\hbar\frac{\partial\psi}{\partial t} = \left[-\frac{\hbar^2}{2m}\nabla^2 + m(U_s)\right]\psi\,. \tag{1}$$

The wave-function is ψ, $\hbar$ is the reduced Planck's constant, m is the mass of the FDM particle. The potential term is U_s, which is the satellite's potential which we will assume that it does not evolve with time. As explained above, we neglect the potential corresponding to FDM, which formally should have appeared in Schrödinger's equation.

The wave-function can be written as a product of a real amplitude and a complex phase:

$$\psi = \sqrt{\rho}e^{i\theta}\,. \tag{2}$$

The square of the real amplitude ρ is the density of the FDM, and the velocity of the $\mathbf{u}$ is the phase of the wave function:

$$\mathbf{u} = \frac{\hbar}{m}\nabla\theta\,. \tag{3}$$

Therefore, the combination of equations 1 and 2, along with an appropriate set of initial conditions allows for the solution of a FDM system and a satellite [26, 27].

The dynamical friction force exerted by the perturbation of the FDM onto the satellite is given by the following expression:

$$F_{DF} = -\bar{\rho} \int_V dV \frac{\rho - \bar{\rho}}{\bar{\rho}} \frac{\mathbf{u_{rel}}}{|\mathbf{u_{rel}}|} \cdot \nabla U \,. \tag{4}$$

We quantify the dynamical friction due to FDM, by defining a dimensionless coefficient which is given by the ratio of a characteristic force using the physical quantities involved in the problem and the dynamical friction force. The reference force is defined as follows:

$$F_{ref} \equiv 4\pi\bar{\rho} \left(\frac{GM}{u_{rel}}\right)^2 \,. \tag{5}$$

M is the mass of the satellite, u_{rel} is the relative of the satellite with respect to the background and $\bar{\rho}$ is the average density of the FDM. Thus, the dimensionless dynamical friction coefficient as follows:

$$C_{rel} \equiv \frac{F_{DF}}{F_{ref}} \,. \tag{6}$$

We further define the Quantum Mach number:

$$M_Q \equiv \frac{u_{rel}\hbar}{GMm} \,. \tag{7}$$

3. Numerical Scheme

For the numerical integration of the governing equation 1 we apply a symplectic integrator, in Fourier space following the formulation of [28]. We separate the kinetic and potential terms of the right-hand side of the Schrödinger equation which are then associated to the Laplacian and the potential operator. The integration method is outline below:

$$\psi \leftarrow \exp\left[-i\frac{\Delta t}{2}\frac{m}{\hbar}U_s\right]\psi, \tag{8a}$$

$$\psi \leftarrow \text{ifft}\left\{\exp\left(-ik^2\Delta t\frac{\hbar}{2m}\right)\text{fft}\left[\psi\right]\right\}, \tag{8b}$$

$$\psi \leftarrow \exp\left[-i\frac{\Delta t}{2}\frac{m}{\hbar}U_s\right]\psi \,. \tag{8c}$$

We denote by fft and ifft the fast Fourier and the inverse fast Fourier transformation, respectively. We step-in-time by Δt, and k is the wavenumber.

We have simulated 2-D and 3-D systems with a typical mode resolution of $N = 256$ in 3-D, and $N = 512$ in the 2-D runs, a time-step $\Delta t = 0.005$ to ensure numerical convergence in all runs. we also run some cases in higher resolution for numerical convergence. The simulation domain size for both the 2-D and the 3-D runs is $L = 50\pi$, unless specified otherwise. We have applied periodic boundary conditions. The initial FDM wavefunction is $\|\psi\| = 1$ so that the density is uniform, and a uniform velocity along the z direction by assuming that the satellite is at rest while the dark matter halo moves. This is implemented by using an appropriate linearly increasing phase.

4. Results

Since our focus is the interaction of the potential with a FDM halo, we will be focusing on two main families of potentials: the spherically symmetric Plummer potential and the logarithmic potential.

The spherically symmetric, Plummer potential [29] given by the following expression

$$U_s = -\frac{GM}{\sqrt{r^2 + R_c^2}}\,. \tag{9}$$

We denote by M the total mass, by R_c the core radius and by r the radial coordinate, measured from the centre.

The axisymmetric logarithmic potentials [30, 31] are described by the following expression

$$U_s = \frac{v_c^2}{2} \ln\left(R^2 + \frac{y^2}{b_y^2} + R_c^2\right)\,. \tag{10}$$

The cylindrical radius is related to the Cartesian coordinates as follows $R^2 = x^2 + z^2$, there the system is axially symmetric round the y-axis. We denote by b_y the ellipticity parameter and v_c is the orbital circular velocity for $r \gg R_c$. The object moves in the z direction. We have also studied another family of potentials where the axis of symmetry is parallel to the direction of motion. These systems are described by the following potential:

$$U_s = \frac{v_c^2}{2} \ln\left(R^2 + \frac{z^2}{b_z^2} + R_c^2\right)\,. \tag{11}$$

Here the axial radius now is $R^2 = x^2 + y^2$. The ellipticity parameter must lie within the range

$$\frac{1}{\sqrt{2}} < b_{y,z} < 1.08\,, \tag{12}$$

to ensure that there are no negative values of energy density [32].

The two-dimensional analogue of the logarithmic system is given in the following expression:

$$U_s = \frac{v_c^2}{2} \ln\left(\frac{y^2}{b_y^2} + \frac{z^2}{b_z^2} + R_c^2\right)\,, \tag{13}$$

where, either b_y, b_z are equal to unity and the parameter varies within the range of appropriate values. other within the range of permitted values. Such models allow faster integration times and provide a qualitative understanding of the behaviour of the system.

In Figures 1 and 2 we plot the FDM density for the Plummer potential for two choices of $M_Q = 1\,, 1/8$. In Figure 3 we plot a series of FDM density for the logarithmic potential where the direction of motion is parallel to the axis of symmetry of the potential.

Next we asses the dimensionless dynamical friction coefficient C_{rel}, for various relative velocities, potentials, ellipticities and directions of motion. Regarding the Plummer potential, Figure 4, we notice that for $M_Q = 1$, C_{rel} is predominantly positive but its value is typically small. On the contrary, for lower M_Q's, the maxima of M_Q are well above unity, but it also has obtains negative

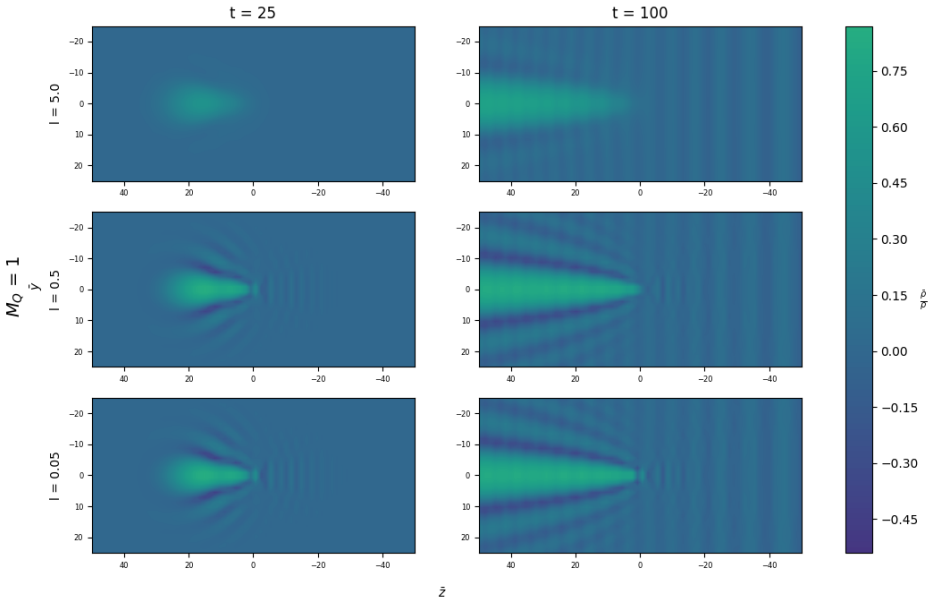

Figure 1: Snapshots of the FDM density contrast at various times for a spherical Plummer potential with $M_Q = 1$ travelling through a FDM for different values of R_C, as indicated on each row.

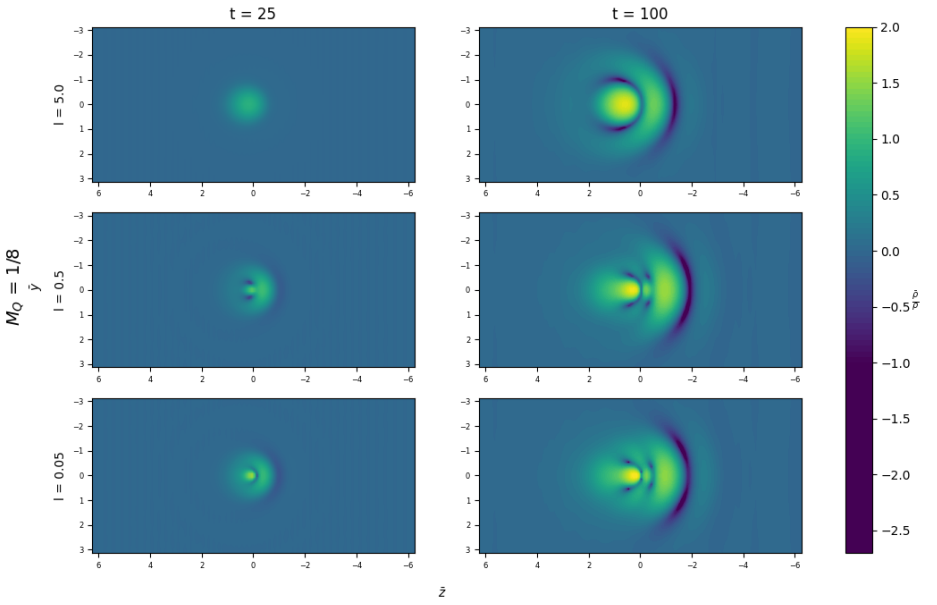

Figure 2: Snapshots of the FDM density ratio at various times for a spherical Plummer potential with $M_Q = 1/8$ travelling through a FDM for different values of R_C, as indicated on each row.

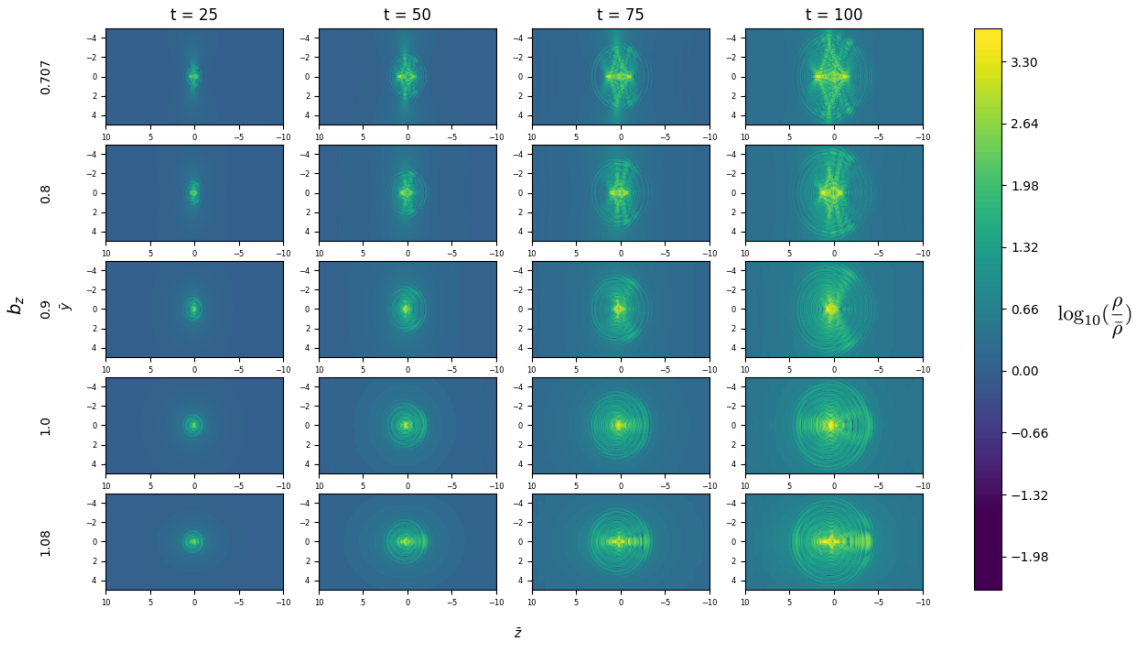

Figure 3: Snapshots of the FDM density ratio over the average density at various times for a logarithmic potential with $R_C = 0.9$ and $M_Q = 0.1$. The rows from top to the bottom have $b_z = 0.707$, 0.8, 0.9, 1, 1.08. The axis of symmetry of the ellipsoid is along the direction of motion. Reproduced from [33].

values. This is representative of the erratic effect of the wake and overdensities lying ahead of the satellite as well as trailing it. Regarding the behaviour of the satellites described by logarithmic potentials, Figures 5 and 6, which are not spherically symmetric, we notice that even though the velocity v_c is the same for all systems, differences by at least a factor of 5 are observed depending on the ellipticity and the direction of motion of the object.

5. Conclusions

While most major studies of dynamical friction due to FDM, so far, have focused on spherically symmetric systems, realistic galaxies, playing the role of satellites and travelling through FDM haloes are unlikely to be spherically symmetric, and are better described by at least axially symmetric or even triaxial potentials. Moreover, extended systems have constant orbital velocities at large distances, and are well described by logarthmic potentials. The simulations we have performed and discussed in these proceedings, demonstrate significant qualitative and quantitative differences between spherically symmetric and axisymmetric systems. These results can be considered in relation to the motion of the Large Magellanic Cloud within the DM halo of the Milky Way. This motion is likely to lead to the creation of a wake [34–36].

If a satellite is not spherically symmetric, the direction of motion of the galaxy with respect to the axis of symmetry, leads to measurable differences on the dynamical friction. It also affects the shape of the wake, which in general trails the underlying mass distribution. Such features cannot be directly observed, yet they may be identified through future maps of DM via gravitational lensing.

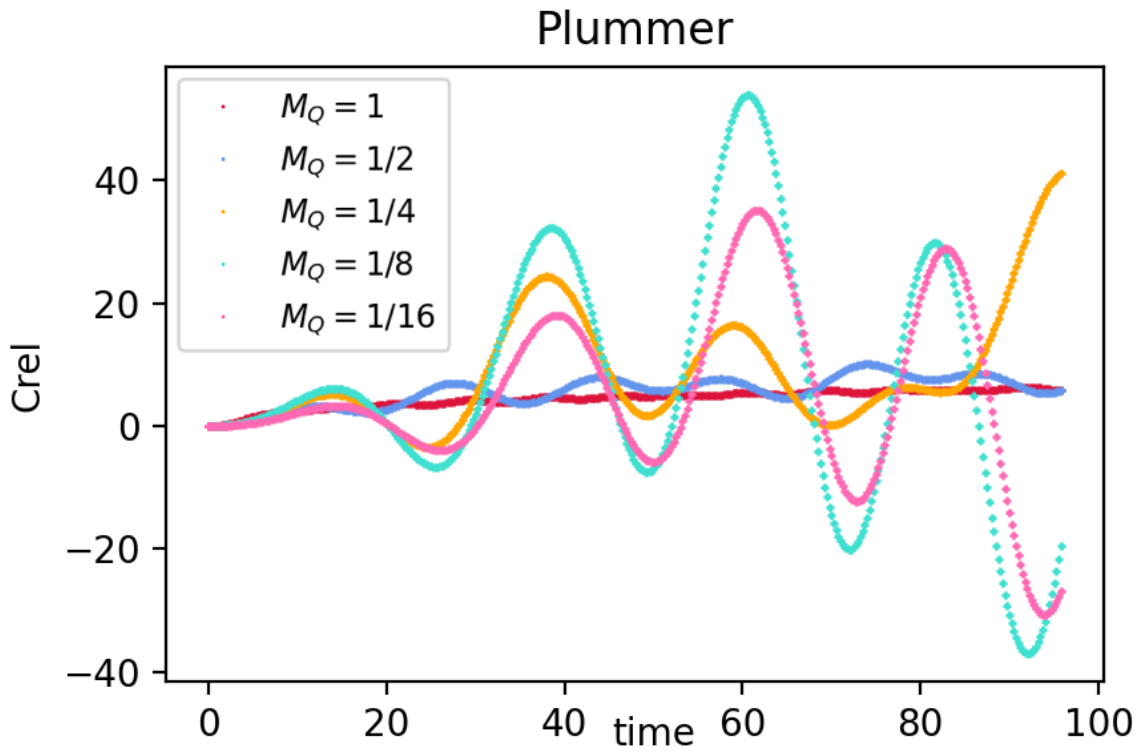

Figure 4: The dynamical friction coefficient C_{rel} as a function of time for Plummer potentials for various values of M_Q. Reproduced from [33].

Finally, we notice that for low velocities the effect of the gravitational force is not always a drag, but it may also lead to acceleration, parallel to the direction of motion. This is due to the fluid nature of the FDM, which may generate overdensities ahead of the satellite.

Acknowledgments

KNG acknowledges funding from grant FK 81641 "Theoretical and Computational Astrophysics", ELKE. The authors acknowledge COST ACTION Cosmic WISPers CA21106 for inspiration on this topic.

References

[1] Zwicky F., 1933, AcHPh, 6, 110

[2] Rubin V. C., Ford W. K., 1970, ApJ, 159, 379. doi:10.1086/150317

[3] Trimble V., 1987, ARA&A, 25, 425. doi:10.1146/annurev.aa.25.090187.002233

[4] Massey R., Kitching T., Richard J., 2010, RPPh, 73, 086901. doi:10.1088/0034-4885/73/8/086901

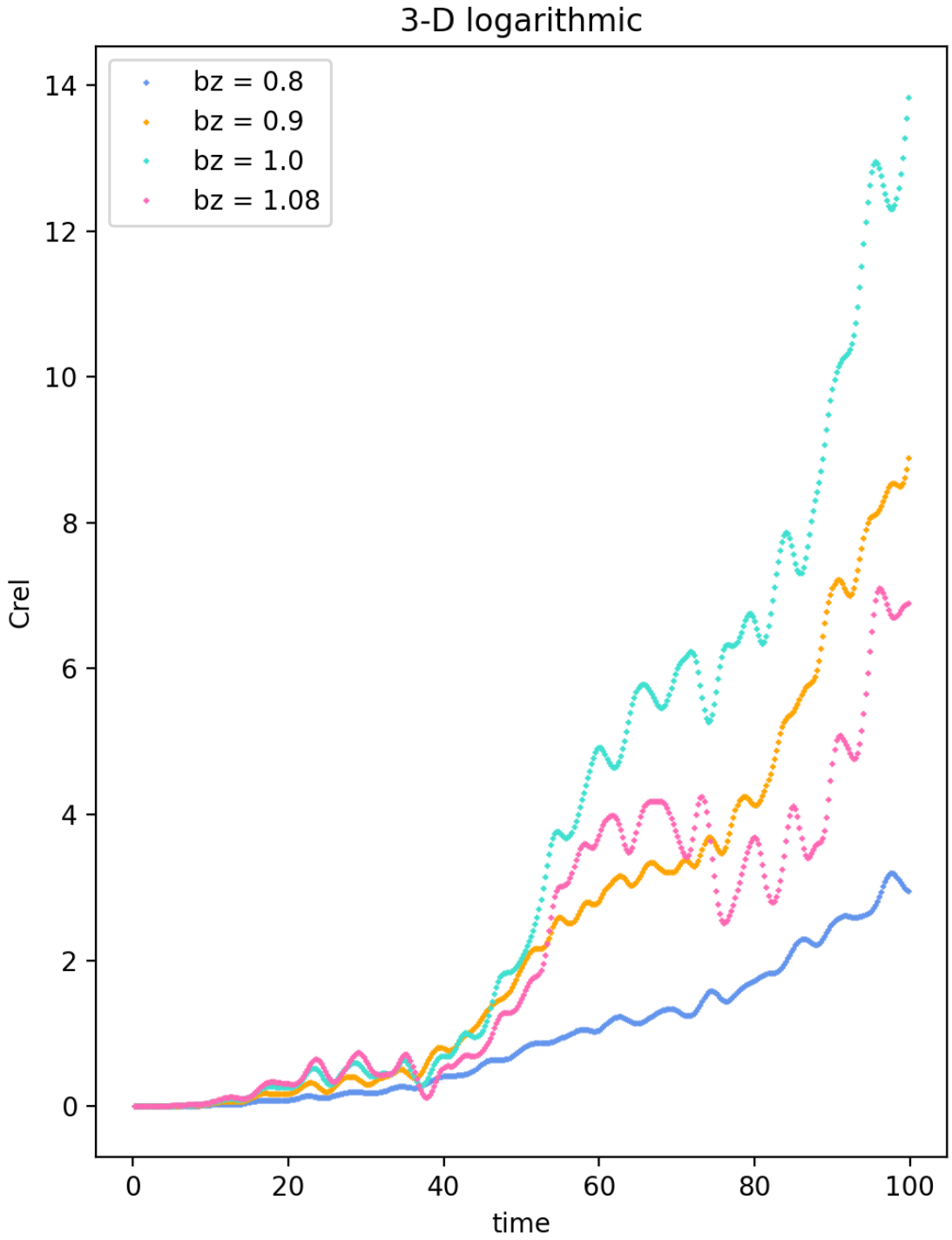

Figure 5: The dynamical friction parameter C_{rel} as a function of time for 3-D logarithmic potentials with various b_z, where the axis of symmetry is parallel to the direction of motion. Reproduced from [33].

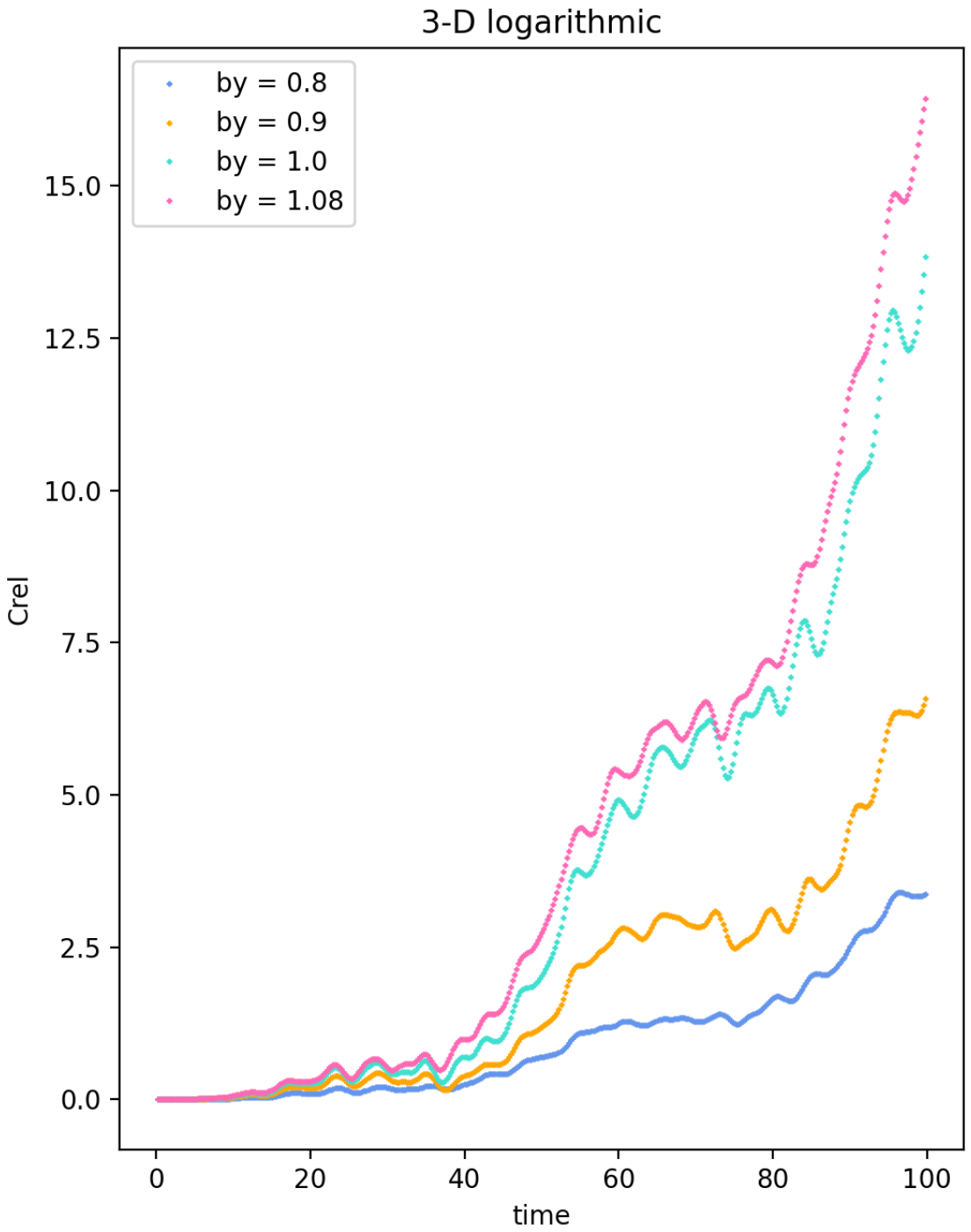

Figure 6: The dynamical friction parameter C_{rel} as a function of time for 3-D logarithmic potentials with various b_z, where the axis of symmetry is parallel to the direction of motion. Reproduced from [33].

[5] Planck Collaboration, Ade P. A. R., Aghanim N., Arnaud M., Ashdown M., Aumont J., Baccigalupi C., et al., 2016, A&A, 594, A13. doi:10.1051/0004-6361/201525830

[6] Clowe D., Gonzalez A., Markevitch M., 2004, ApJ, 604, 596. doi:10.1086/381970

[7] Eisenstein D. J., Zehavi I., Hogg D. W., Scoccimarro R., Blanton M. R., Nichol R. C., Scranton R., et al., 2005, ApJ, 633, 560. doi:10.1086/466512

[8] Planck Collaboration, Aghanim N., Akrami Y., Ashdown M., Aumont J., Baccigalupi C., Ballardini M., et al., 2020, A&A, 641, A6. doi:10.1051/0004-6361/201833910

[9] Jungman G., Kamionkowski M., Griest K., 1996, PhR, 267, 195. doi:10.1016/0370-1573(95)00058-5

[10] Espinosa J. R., Racco D., Riotto A., 2018, PhRvL, 120, 121301. doi:10.1103/PhysRevLett.120.121301

[11] Alcock C., Allsman R. A., Alves D. R., Axelrod T. S., Becker A. C., Bennett D. P., Cook K. H., et al., 2000, ApJ, 542, 281. doi:10.1086/309512

[12] Freese K., 1986, PhLB, 167, 295. doi:10.1016/0370-2693(86)90349-7

[13] Milgrom M., 1983, ApJ, 270, 365. doi:10.1086/161130

[14] Baldeschi, M., Gelmini, G. & Ruffini, R. On massive fermions and bosons in galactic halos. *Physics Letters B*. **122**, 221-224 (1983), https://www.sciencedirect.com/science/article/pii/0370269383906883

[15] Ferreira, E. Ultra-light dark matter. *The Astronomy And Astrophysics Review*. **29** (2021,9), https://doi.org/10.1007

[16] Ringwald A., 2012, PDU, 1, 116. doi:10.1016/j.dark.2012.10.008

[17] Hu W., Barkana R., Gruzinov A., 2000, PhRvL, 85, 1158. doi:10.1103/PhysRevLett.85.1158

[18] Du X., Behrens C., Niemeyer J. C., 2017, MNRAS, 465, 941. doi:10.1093/mnras/stw2724

[19] Moore B., 1994, Natur, 370, 629. doi:10.1038/370629a0

[20] Chandrasekhar S., 1943, ApJ, 97, 255. doi:10.1086/144517

[21] Chandrasekhar S., 1943, ApJ, 97, 263. doi:10.1086/144518

[22] Chandrasekhar S., 1943, ApJ, 98, 54. doi:10.1086/144544

[23] Hui L., 2021, ARA&A, 59, 247. doi:10.1146/annurev-astro-120920-010024

[24] Lancaster L., Giovanetti C., Mocz P., Kahn Y., Lisanti M., Spergel D. N., 2020, JCAP, 2020, 001. doi:10.1088/1475-7516/2020/01/001

[25] Traykova D., Clough K., Helfer T., Berti E., Ferreira P. G., Hui L., 2021, PhRvD, 104, 103014. doi:10.1103/PhysRevD.104.103014

[26] Mocz P., Fialkov A., Vogelsberger M., Becerra F., Amin M. A., Bose S., Boylan-Kolchin M., et al., 2019, PhRvL, 123, 141301. doi:10.1103/PhysRevLett.123.141301

[27] Mocz P., Fialkov A., Vogelsberger M., Becerra F., Shen X., Robles V. H., Amin M. A., et al., 2020, MNRAS, 494, 2027. doi:10.1093/mnras/staa738

[28] Mocz P., Vogelsberger M., Robles V. H., Zavala J., Boylan-Kolchin M., Fialkov A., Hernquist L., 2017, MNRAS, 471, 4559. doi:10.1093/mnras/stx1887

[29] Plummer H. C., 1911, MNRAS, 71, 460. doi:10.1093/mnras/71.5.460

[30] Richstone D. O., 1980, ApJ, 238, 103. doi:10.1086/157963

[31] Binney J., 1981, MNRAS, 196, 455. doi:10.1093/mnras/196.3.455

[32] Evans N. W., 1993, MNRAS, 260, 191. doi:10.1093/mnras/260.1.191

[33] Vitsos A., Gourgouliatos K. N., 2022, arXiv, arXiv:2211.06752. doi:10.48550/arXiv.2211.06752

[34] Garavito-Camargo N., Besla G., Laporte C. F. P., Johnston K. V., Gómez F. A., Watkins L. L., 2019, ApJ, 884, 51. doi:10.3847/1538-4357/ab32eb

[35] Garavito-Camargo N., Besla G., Laporte C. F. P., Price-Whelan A. M., Cunningham E. C., Johnston K. V., Weinberg M., et al., 2021, ApJ, 919, 109. doi:10.3847/1538-4357/ac0b44

[36] Koposov S. E., Erkal D., Li T. S., Da Costa G. S., Cullinane L. R., Ji A. P., Kuehn K., et al., 2023, MNRAS.tmp. doi:10.1093/mnras/stad551